Journal of Sound and Vibration (2001) **240**(2), 219–240
doi:10.1006/jsvi.2000.3214, available online at http://www.idealibrary.com on IDEAL®

ON THE RECONSTRUCTION OF A DAMPED VIBRATING SYSTEM FROM TWO COMPLEX SPECTRA, PART 2: EXPERIMENT

E. FOLTÊTE

Laboratoire de Mécanique Appliquée R. Chaléat, 24 rue de l'Epitaphe, 25000 Besançon, France.
E-mail: emmanuel.foltete@univ-fcomte.fr

G. M. L. GLADWELL

Department of Civil Engineering, University of Waterloo, Waterloo, Ontario, Canada N2L 3G1.
E-mail: ggladwell@uwaterloo.ca

AND

G. LALLEMENT

Laboratoire de Mécanique Appliquée R. Chaléat, 24 rue de l'Epitaphe, 25000 Besançon, France.
E-mail: gerard.lallement@univ-fcomte.fr

(*Received* 22 *November* 1999, *and in final form* 18 *April* 2000)

This experimental–theoretical paper discusses whether, and how accurately, the mass, damping and stiffness matrices for a purportedly two-degree-of-freedom (2-d.o.f.) system may be reconstructed from the measured complex eigenvalues and/or eigenvectors. The system consists of two parallel cantilevered beams with end masses connected by a third, curved beam. Three procedures are used to reconstruct the matrices: the modal (M) method using real natural frequencies, real modes and modal damping factors; Danek's (D) reconstruction from complex eigenvalues and eigenvectors; a reconstruction (E) from complex eigenvalues of the original and constrained system. It is shown that the damping matrix constructed via D is extremely sensitive to errors in the phases of the complex eigenvectors. The reconstruction via E uses only eigenvalues which can be measured much more reliably than eigenvectors.

1. INTRODUCTION

It is now almost universal practice to model a damped vibrating system by a matrix equation of the form

$$\mathbf{M}\ddot{\mathbf{q}}(t) + \mathbf{B}\dot{\mathbf{q}}(t) + \mathbf{K}\mathbf{q}(t) = \mathbf{f}(t). \tag{1}$$

Here **M**, **B**, **K** are the mass, damping and stiffness matrices, assumed to be symmetric and positive definite. There are now well-established procedures for constructing **M**, **K**, using finite element methods or whatever, for a given mechanical system, and for updating them so that computations made with them agree with actual measurements; see Friswell and Mottershead [1] or Mottershead and Friswell [2] for a review of the literature. The situation regarding **B**, the damping matrix, is quite different. Every actual vibrating system

0022-460X/01/070219 + 22 $35.00/0

experiences damping, but its origin is often ill-defined; it arises from structural joints, from damping devices which have been deliberately applied to the system, from bearings and other contacts between moving parts, etc. Provided that the damping is small (in some sense) and the natural frequencies of the structure are well separated, it is usual to suppose that the damping is viscous, and that it can be represented by modal damping factors. This is equivalent to assuming that the three matrices **M**, **B**, **K** can be simultaneously diagonalized; for conditions under which it is possible (see, e.g., reference [3]). In this situation, the damping is said to be modal; the mode shapes of the damped system are then the same as those of the undamped system; the only difference which the damping produces is in the eigenvalues of the characteristic equation

$$det(\mathbf{M}\lambda^2 + \mathbf{B}\lambda + \mathbf{K}) = \mathbf{0}, \tag{2}$$

instead of being purely imaginary, as in the undamped case, they become complex, with small non-positive real parts. If it is assumed that the damping is modal, then the problem of reconstructing **B** from complex eigenvalues is straightforward: there exists a non-singular matrix **X** of (real) mode shapes such that

$$\mathbf{X}^T(\mathbf{M}\lambda^2 + \mathbf{B}\lambda + \mathbf{K})\mathbf{X} = (\lambda^2\mathbf{I} + \lambda\beta + \mathbf{\Omega}^2), \tag{3}$$

where β and Ω^2 are diagonal, i.e.,

$$\beta = diag(\beta_1, \beta_2, \ldots, \beta_n), \quad \Omega^2 = diag(\Omega_1^2, \Omega_2^2, \ldots, \Omega_n^2). \tag{4}$$

If the complex eigenvalue pairs are $(\lambda_j, \bar{\lambda}_j)_1^n$, then

$$\lambda^2 + \beta_j\lambda + \Omega_j^2 = (\lambda - \lambda_j)(\lambda - \bar{\lambda}_j), \tag{5}$$

i.e.,

$$\beta_j = -\lambda_j - \bar{\lambda}_j, \quad \Omega_j^2 = \lambda_j\bar{\lambda}_j = |\lambda_j|^2 \tag{6, 7}$$

and

$$\mathbf{B} = \mathbf{X}^{-\mathrm{T}}\beta\mathbf{X}^{-1}. \tag{8}$$

The question which we ask, and attempt to answer in this paper is"*Is it possible to construct all three matrices* **M**, **B**, **K** *from experimental measurements of the behaviour of the system, without assuming that the damping is modal* ?". We note that this question, as also the reconstruction of **B** from modal-damping factors, is based on the presupposition that it is possible to define *n*, the number of degrees of freedom of the system. The best that can be said about an actual system is that, *in a specified frequency range*, it behaves roughly as though it were a system with a certain number of degrees of freedom (d.o.f.). The first step in any experimental investigation must therefore be the choice of a system with *n* d.o.f. in a certain frequency range. After considering a number of possibilities we chose the system shown in Figure 1. In the absence of (extra) damping (and its residual damping is very small), its first three natural frequencies are 14·9, 38·6, 101·5 Hz. Since the third frequency is well separated from the first two, the system can be treated as a two-degree-of-freedom (2-d.o.f.) system for the limited range 0–50 Hz. Different levels of viscous damping were introduced through two independent collocated velocity feedback devices. The following

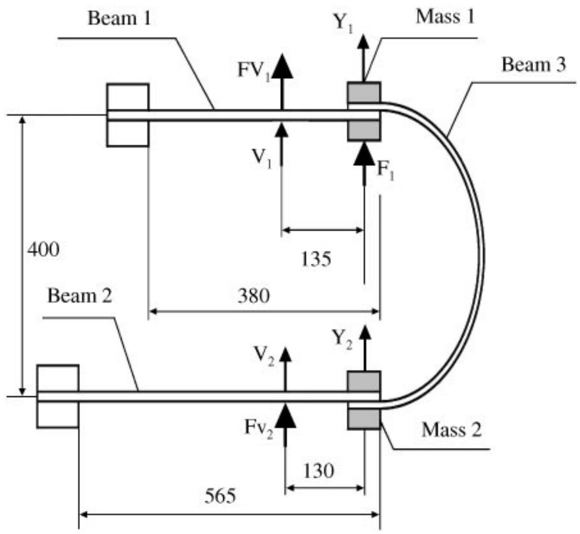

Figure 1. Experimental set-up.

measurements were made: the two complex eigenvalues and eigenvectors; the single complex eigenvalue of the system when the mass m_2 was fixed.

The plan of the paper is as follows: section 2 recalls the well-known reconstruction of **M**, **K** from real modes; section 3 describes Danek's generalization of the reconstruction of **M**, **B**, **K** from complex modes; and section 4 gives an account of the specialization of the theory given in Gladwell [4] to small damping and $n = 2$. Section 5 describes the experimental procedure.

2. RECONSTRUCTION FROM REAL MODES

There is now a well-established procedure for finding the real modes of a damped system, i.e., the modes that the system would have if there were no damping. The details of the experimental procedure and postprocessing analysis may be found in reference [5].

The real modes $\mathbf{x}_i$ and real natural frequencies ω_i satisfy

$$(\mathbf{K} - \omega_i^2\mathbf{M})\mathbf{x}_i = 0. \tag{9}$$

If $\mathbf{X} = [\mathbf{x}_1, \mathbf{x}_2, \ldots, \mathbf{x}_n]$ then equations (9) for $i = 1, 2, \ldots, n$ yield

$$\mathbf{KX}=\mathbf{MX}\Omega^2, \tag{10}$$

where $\Omega^2 = diag(\omega_1^2, \omega_2^2, \ldots, \omega_n^2)$. The orthonormality of the modes w.r.t. the mass matrix now yields

$$\mathbf{X}^{\mathrm{T}}\mathbf{MX} = \mathbf{I}, \quad \mathbf{X}^{\mathrm{T}}\mathbf{KX} = \Omega^2. \tag{11}$$

These equations may be solved for **M**, **K**:

$$\mathbf{M} = \mathbf{X}^{-\mathrm{T}}\mathbf{X}^{-1}, \quad \mathbf{K} = \mathbf{X}^{-\mathrm{T}}\Omega^2\mathbf{X}^{-1}. \tag{12}$$

These may be written in the alternative form

$$\mathbf{M}^{-1} = \mathbf{X}\mathbf{X}^{\mathrm{T}}, \quad \mathbf{K}^{-1} = \mathbf{X}\Omega^{-2}\mathbf{X}^{\mathrm{T}}. \tag{13}$$

We make two brief comments regarding this reconstruction; one positive and one negative: in practice, for small n, say $n \leqslant 4$, the condition number of the matrix $\mathbf{X}$ is small; as a consequence the reconstructed $\mathbf{K}$ and $\mathbf{M}$ are reasonably insensitive to small errors in the measured modes; the matrices $\mathbf{M}$ and $\mathbf{K}$ constructed from equation (12) will generally be fully populated, even though there might be *a priori* reasons for assuming that they should have a certain structure or connectivity of non-zero and zero terms; this is where model updating has its place. Model updating provides a procedure for finding a matrix with the appropriate connectivity near, in some sense, to the reconstructed matrices. In the particular case $n = 2$ of course, there is no need for updating because $\mathbf{M}$, $\mathbf{K}$ would be expected, on physical grounds, to be fully populated.

3. DANEK'S RECONSTRUCTION

We recall the analysis from Danek [6]. The free vibration equations for $\mathbf{q}_j(t) = \mathbf{y}_j \exp(s_j t)$ are

$$(\mathbf{M}\lambda_j^2 + \mathbf{B}\lambda_j + \mathbf{K})\mathbf{y}_j = \mathbf{0}. \tag{14}$$

These are written in the form

$$\begin{bmatrix} -\mathbf{K} & \mathbf{0} \\ \mathbf{0} & \mathbf{M} \end{bmatrix}\begin{bmatrix} \mathbf{y}_j \\ \lambda_j \mathbf{y}_j \end{bmatrix} = \lambda_j \begin{bmatrix} \mathbf{B} & \mathbf{M} \\ \mathbf{M} & \mathbf{0} \end{bmatrix}\begin{bmatrix} \mathbf{y}_j \\ \lambda_j \mathbf{y}_j \end{bmatrix}, \tag{15}$$

and then assembled, as in equation (10), into one equation

$$\mathbf{A}\mathbf{X} = \mathbf{C}\mathbf{X}\tilde{\mathbf{\Lambda}}, \tag{16}$$

where

$$\mathbf{A} = \begin{bmatrix} -\mathbf{K} & \mathbf{0} \\ \mathbf{0} & \mathbf{M} \end{bmatrix}, \quad \mathbf{C} = \begin{bmatrix} \mathbf{B} & \mathbf{M} \\ \mathbf{M} & \mathbf{0} \end{bmatrix}, \tag{17}$$

$$\mathbf{X} = \begin{bmatrix} \mathbf{Y} & \overline{\mathbf{Y}} \\ \mathbf{Y}\mathbf{\Lambda} & \overline{\mathbf{Y}\mathbf{\Lambda}} \end{bmatrix}, \quad \tilde{\mathbf{\Lambda}} = \begin{bmatrix} \mathbf{\Lambda} & \\ & \overline{\mathbf{\Lambda}} \end{bmatrix}. \tag{18}$$

We note that $\mathbf{A}$, $\mathbf{C}$ are symmetric matrices of order $2n$, and for small damping the eigenvalues and eigenvectors both come in complex conjugate pairs: $(\lambda_j, \mathbf{y}_j)$ and $(\bar{\lambda}_j, \bar{\mathbf{y}}_j)$. Now the columns of $\mathbf{X}$ are orthogonal w.r.t. $\mathbf{C}$, so that

$$\mathbf{X}^{\mathrm{T}}\mathbf{C}\mathbf{X} = \mathbf{I}, \quad \mathbf{X}^{\mathrm{T}}\mathbf{A}\mathbf{X} = \tilde{\mathbf{\Lambda}}, \tag{19}$$

which yield

$$\mathbf{C}^{-1} = \mathbf{X}\mathbf{X}^{\mathrm{T}}, \quad \mathbf{A}^{-1} = \mathbf{X}\tilde{\mathbf{\Lambda}}^{-1}\mathbf{X}^{\mathrm{T}}. \tag{20}$$

We now examine these equations when **A**, **C** and **X** are replaced by the expressions in equations (17) and (18). We find

$$\mathbf{C}^{-1} = \begin{bmatrix} \mathbf{0} & \mathbf{M}^{-1} \\ \mathbf{M}^{-1} & -\mathbf{M}^{-1}\mathbf{B}\mathbf{M}^{-1} \end{bmatrix} = \begin{bmatrix} \mathbf{Y} & \bar{\mathbf{Y}} \\ \mathbf{Y}\mathbf{\Lambda} & \overline{\mathbf{Y}\mathbf{\Lambda}} \end{bmatrix} \begin{bmatrix} \mathbf{Y}^{\mathrm{T}} & \mathbf{\Lambda}\mathbf{Y}^{\mathrm{T}} \\ \bar{\mathbf{Y}}^{\mathrm{T}} & \overline{\mathbf{\Lambda}\mathbf{Y}^{\mathrm{T}}} \end{bmatrix}, \tag{21}$$

$$\mathbf{A}^{-1} = \begin{bmatrix} -\mathbf{K}^{-1} & \mathbf{0} \\ \mathbf{0} & \mathbf{M}^{-1} \end{bmatrix} = \begin{bmatrix} \mathbf{Y} & \bar{\mathbf{Y}} \\ \mathbf{Y}\mathbf{\Lambda} & \overline{\mathbf{Y}\mathbf{\Lambda}} \end{bmatrix} \begin{bmatrix} \mathbf{\Lambda}^{-1} & \\ & \bar{\mathbf{\Lambda}}^{-1} \end{bmatrix} \begin{bmatrix} \mathbf{Y}^{\mathrm{T}} & \mathbf{\Lambda}\mathbf{Y}^{\mathrm{T}} \\ \bar{\mathbf{Y}}^{\mathrm{T}} & \overline{\mathbf{\Lambda}\mathbf{Y}^{\mathrm{T}}} \end{bmatrix}, \tag{22}$$

and thus

$$\mathbf{M}^{-1} = \mathbf{Y}\mathbf{\Lambda}\mathbf{Y}^{\mathrm{T}} + \overline{\mathbf{Y}\mathbf{\Lambda}\mathbf{Y}^{\mathrm{T}}} = 2\,\mathrm{Re}(\mathbf{Y}\mathbf{\Lambda}\mathbf{Y}^{\mathrm{T}}), \tag{23}$$

$$\mathbf{K}^{-1} = 2\,\mathrm{Re}(\mathbf{Y}\mathbf{\Lambda}^{-1}\mathbf{Y}^{\mathrm{T}}), \tag{24}$$

$$\mathbf{B} = -2\mathbf{M}\,\mathrm{Re}(\mathbf{Y}\mathbf{\Lambda}^{2}\mathbf{Y}^{\mathrm{T}})\mathbf{M}, \quad \mathbf{0} = \mathrm{Re}(\mathbf{Y}\mathbf{Y}^{\mathrm{T}}). \tag{25, 26}$$

Equations (23) and (24) provide an alternative to the real reconstruction equations (13); equation (25) yields the damping matrix **B**; the last equation (26) gives an orthogonality condition which the complex modes must satisfy if they are to be modes of a viscously damped system.

The most important equation is equation (25). However, we found that **B** constructed from experimental measured complex modes was extremely sensitive to small changes in the complex mode shapes as we will discuss later.

4. RECONSTRUCTION FROM COMPLEX EIGENVALUES

In a recent paper, Gladwell [4] showed how a system made up of lumped spring-mass-damper systems set in parallel could be constructed from its n pairs of complex eigenvalues, and the $(n-1)$ pairs of eigenvalues of the system when the end mass is fixed. We use this theory, specialized to the case $n = 2$ and to small damping.

There is an important matter which has not yet been properly clarified for damped systems. It is well known that if an undamped (i.e., conservative) system is subjected to a displacement-type constraint, then its eigenvalues will *interlace* the eigenvalues of the original system. This interlacing condition plays a fundamental role in inverse problem for conservative systems: a necessary condition for the existance of a system with eigenvalues $(\lambda_i)_1^n$, and such that, when it is constrained, its eigenvalues are $(\mu_i)_1^{n-1}$, is

$$\lambda_i \leqslant \mu_i \leqslant \lambda_{i+1}, \quad i = 1, 2, \ldots, n-1. \tag{27}$$

The interlacing condition is simple: there is one double-sided inequality for each μ_i. For damped systems, the situation is quite different: suppose a damped system has complex conjugate pairs of eigenvalues $(\lambda_i, \bar{\lambda}_i)_1^n$. The conditions which must be satisfied by pairs $(\mu_i, \bar{\mu}_i)_1^{n-1}$, for them to be possible eigenvalues of the system when it is subjected to a constraint, are not simple double-sided inequalities. Now the eigenvalues lie in the complex plane and, unlike the real line, this cannot be ordered. Nor are there individual conditions on the μ_i; the conditions involve the whole set of eigenvalues $(\mu_i, \bar{\mu}_i)_1^{n-1}$, as shown in reference [4]. When $n = 2$, there is just one set of conditions on $\mathrm{Re}(\mu_1)$, and it is possible to show these conditions graphically in the three-space spanned by the real parts of λ_1, λ_2, and μ_1. The conditions are shown in equations (59) and (60) and verified for the experimental results in section 8.

For the 2-d.o.f. model of the experimental system we expect the matrices to have the forms

$$\mathbf{K} = \begin{bmatrix} k_1 + k_{12} & -k_{12} \\ -k_{12} & k_{12} + k_2 \end{bmatrix}, \quad \mathbf{B} = \begin{bmatrix} b_1 + b_{12} & -b_{12} \\ -b_{12} & b_{12} + b_2 \end{bmatrix}, \quad \mathbf{M} = \begin{bmatrix} m_{11} & m_{12} \\ m_{12} & m_{22} \end{bmatrix}. \tag{28}$$

Both **K** and **B** are positive definite, diagonally dominant matrices with negative off-diagonal terms; **M** is positive definite and has positive off-diagonal term m_{12}. We first reduce the problem to standard form by factorising **M**:

$$\mathbf{M} = \mathbf{L}\mathbf{L}^{\mathrm{T}}, \quad \mathbf{L}^{-1}\mathbf{K}\mathbf{L}^{-\mathrm{T}} = \mathbf{A}, \quad \mathbf{L}^{-1}\mathbf{B}\mathbf{L}^{-\mathrm{T}} = \mathbf{C}, \tag{29}$$

where

$$\mathbf{L} = \begin{bmatrix} l_{11} & 0 \\ l_{21} & l_{22} \end{bmatrix}. \tag{30}$$

The matrices **A**, **C** will have the forms

$$\mathbf{A} = \begin{bmatrix} \sigma_1^2 & -a \\ -a & \sigma_2^2 \end{bmatrix}, \quad \mathbf{C} = \begin{bmatrix} c_1 & -d \\ -d & c_2 \end{bmatrix}. \tag{31}$$

This means that the free vibration equation

$$(\mathbf{M}\lambda^2 + \mathbf{B}\lambda + \mathbf{K})\mathbf{y} = \mathbf{0} \tag{32}$$

reduces to

$$(\mathbf{I}\lambda^2 + \mathbf{C}\lambda + \mathbf{A})\mathbf{x} = \mathbf{0}, \tag{33}$$

where

$$\mathbf{y} = \mathbf{L}^{-\mathrm{T}}\mathbf{x} \quad \text{or} \quad \mathbf{x} = \mathbf{L}^{\mathrm{T}}\mathbf{y}. \tag{34}$$

We note that this last equation is

$$\begin{bmatrix} x_1 \\ x_2 \end{bmatrix} = \begin{bmatrix} l_{11} & l_{21} \\ 0 & l_{22} \end{bmatrix} \begin{bmatrix} y_1 \\ y_2 \end{bmatrix}, \tag{35}$$

so that $y_2 = 0$ implies $x_2 = 0$.

Clearly, we cannot expect to be able to calculate the three matrices **M**, **B**, **K** from the eigenvalues alone. However, we can calculate **A**, **C**. More precisely, as shown later, we can compute **A** from the two *undamped* eigenvalues of the system and the one *undamped* eigenvalue of the system when $y_2 = 0$; and we can compute **C** from the corresponding *damped* eigenvalues. If we know **M**, from say (real) modal data, then we can compute **L** from equation (29a) and then find

$$\mathbf{K} = \mathbf{L}\mathbf{A}\mathbf{L}^{\mathrm{T}}, \quad \mathbf{B} = \mathbf{L}\mathbf{C}\mathbf{L}^{\mathrm{T}}. \tag{36}$$

First, consider the calculation of **A**. Suppose the natural frequencies of the system in the absence of damping are ω_1, ω_2, and for the constrained system, σ_1. Then

$$\lambda_1 = \mathrm{i}\,\omega_1, \overline{\lambda}_1 = -\,\mathrm{i}\,\omega_1, \quad \lambda_2 = \mathrm{i}\,\omega_2, \quad \overline{\lambda}_2 = -\,\mathrm{i}\,\omega_2, \quad \mu_1 = \mathrm{i}\,\sigma_1, \quad \bar{\mu}_1 = -\mathrm{i}\,\sigma_1 \tag{37}$$

and

$$\begin{aligned} det(\mathbf{A} + \lambda^2\mathbf{I}) &= (\sigma_1^2 + \lambda^2)(\sigma_2^2 + \lambda^2) - a^2 \\ &= (\lambda - \mathrm{i}\,\omega_1)(\lambda + \mathrm{i}\,\omega_1)(\lambda - \mathrm{i}\,\omega_2)(\lambda + \mathrm{i}\,\omega_2) \\ &= (\lambda^2 + \omega_1^2)(\lambda^2 + \omega_2^2). \end{aligned} \tag{38}$$

Thus,

$$\sigma_1^2 + \sigma_2^2 = \omega_1^2 + \omega_2^2, \quad \sigma_1^2\sigma_2^2 - a^2 = \omega_1^2\omega_2^2. \tag{39}$$

Since $\omega_1 < \sigma_1 < \omega_2$ we may introduce an angle θ such that $0 < \theta < \pi/2$, and write

$$\sigma_1^2 = \omega_1^2 \cos^2\theta + \omega_2^2 \sin^2\theta, \tag{40}$$

then

$$\sigma_2^2 = \omega_1^2 + \omega_2^2 - \sigma_1^2 = \omega_1^2 \sin^2\theta + \omega_2^2 \cos^2\theta \tag{41}$$

and

$$a = (\omega_2^2 - \omega_1^2)\cos\theta\sin\theta. \tag{42}$$

Now consider the damped system. Suppose the damped eigenvalues of the system are $(\lambda_1, \overline{\lambda}_1)$, $(\lambda_2, \overline{\lambda}_2)$, and of the constrained system $(\mu_1, \bar{\mu}_1)$, where

$$\lambda_1 = -\,s_1 + \mathrm{i}\,\omega_1, \quad \lambda_2 = -\,s_2 + \mathrm{i}\,\omega_2, \quad \mu_1 = -\,t_1 + \mathrm{i}\,\sigma_1, \tag{43}$$

and s_1, s_2, t_1 are small and positive. Then

$$\begin{aligned} &(\lambda^2 + c_1\lambda + \sigma_1^2)(\lambda^2 + c_2\lambda + \sigma_2^2) - (a + \lambda d)^2 \\ &\equiv (\lambda - \lambda_1)(\lambda - \overline{\lambda}_1)(\lambda - \lambda_2)(\lambda - \overline{\lambda}_2), \end{aligned} \tag{44}$$

and

$$\lambda^2 + c_1\lambda + \sigma_1^2 = (\lambda - \mu_1)(\lambda - \bar{\mu}_1). \tag{45}$$

Equation (45) gives

$$c_1 = -\,\mu_1 - \bar{\mu}_1 = 2t_1, \tag{46}$$

while equation (44) gives

$$c_1 + c_2 = -\,\lambda_1 - \overline{\lambda}_1 - \lambda_2 - \overline{\lambda}_2 = 2s_1 + 2s_2, \tag{47}$$

and thus

$$c_2 = 2s_1 + 2s_2 - 2t_1 \,. \tag{48}$$

Now putting $\lambda = \mu_1$ in equation (44) we find

$$(a + \mu_1 d)^2 = -(\mu_1 - \lambda_1)(\mu_1 - \overline{\lambda}_1)(\mu_1 - \lambda_2)(\mu_1 - \overline{\lambda}_2)\,. \tag{49}$$

Upon inserting the expressions for $\lambda_1, \lambda_2, \mu_1$ and taking the square root we find, to the first order,

$$d = (s_2 - t_1)\tan\theta - (s_1 - t_1)\cot\theta\,. \tag{50}$$

Equations (46), (48) and (50) give **C**, and then

$$\mathbf{B} = \mathbf{LCL}^{\mathrm{T}} = \begin{bmatrix} l_{11} & \\ l_{21} & l_{22} \end{bmatrix} \begin{bmatrix} c_1 & -d \\ -d & c_2 \end{bmatrix} \begin{bmatrix} l_{11} & l_{21} \\ & l_{22} \end{bmatrix}. \tag{51}$$

On equating this to **B** given in equation (28) we find

$$b_{12} = l_{11}(l_{22}d - l_{21}c_1), \quad b_1 = l_{11}\{(l_{11} + l_{21})c_1 - l_{22}d\}, \tag{52, 53}$$

$$b_2 = (l_{11} + l_{21})(l_{21}c_1 - l_{22}d) + l_{22}(l_{22}c_2 - l_{21}d)\,. \tag{54}$$

Since m_{11}, m_{12}, m_{22} are all positive and **M** is positive definite, l_{11}, l_{21}, l_{22} are all positive. The conditions that b_1, b_2, b_{12} be all positive lead to the inequalities

$$\frac{l_{21}}{l_{22}} < \frac{d}{c_1}, \quad \frac{l_{11} + l_{21}}{l_{22}} > \frac{d}{c_1}, \quad \frac{l_{11} + l_{21}}{l_{22}} < \frac{l_{22}c_2 - l_{21}d}{l_{22}d - l_{21}c_1}\,. \tag{55}$$

For consistency, these inequalities require

$$d > 0, \quad c_1c_2 - d^2 > 0\,. \tag{56}$$

After some algebra we find

$$\sin^2\theta\cos^2\theta(d^2 - c_1c_2) = t_1^2 - 2t_1(s_1\cos^2\theta + s_2\sin^2\theta) + (s_1\cos^2\theta + s_2\sin^2\theta)^2. \tag{57}$$

Thus, t_1 must lie between the roots of the quadratic on the right-hand side; this leads to the inequalities

$$(s_1^{1/2}\cos\theta - s_2^{1/2}\sin\theta)^2 < t_1 < (s_1^{1/2}\cos\theta + s_2^{1/2}\sin\theta)^2\,. \tag{58}$$

To show the feasible regions for s_1, s_2, t_1 we put $s_1^{1/2} = x$, $s_2^{1/2} = y$, $t_1^{1/2} = z$, then $d > 0$ and equation (58) become

$$y^2\sin^2\theta - x^2\cos^2\theta + z^2\cos 2\theta > 0, \tag{59}$$

$$|x\cos\theta - y\sin\theta| < z < x\cos\theta + y\sin\theta. \tag{60}$$

These state that $P(x, y, z)$ must lie in a region bounded by two planes and a cone, as shown later in Figure 7. When these conditions are satisfied equations (52–54) will yield b_1, b_2, b_{12} all positive.

5. SENSITIVITY ANALYSIS

In this section, we attempt to explain why the damping matrix reconstructed via Danek's method is so unreliable. To do so we estimate the sensitivities of terms in the mass, stiffness and damping matrices to changes in the phase of the complex modes.

In Danek's reconstruction, the inverse of the mass matrix is given by equation (23). Suppose that $\mathbf{M}$ is diagonal; this simplifies the analysis without significantly affecting the conclusions. Then

$$\mathbf{M} = diag(m_1, m_2), \quad \mathbf{M}^{-1} = 2\,\mathrm{Re}(\mathbf{Y}\boldsymbol{\Lambda}\mathbf{Y}^{\mathrm{T}}). \tag{61}$$

Thus,

$$m_p^{-1} = 2\,\mathrm{Re}(\lambda_1 y_{p1}^2 + \lambda_2 y_{p2}^2), \quad p = 1, 2, \ldots, n. \tag{62}$$

Suppose that the phase of y_{pq} is ϕ_{pq}, so that

$$y_{pq} = a_{pq} \exp(\mathrm{i}\,\phi_{pq}). \tag{63}$$

Then, since $\lambda_1 = -s_1 + \mathrm{i}\,\omega_1$, $\lambda_2 = -s_2 + \mathrm{i}\,\omega_2$, we have

$$m_p^{-1} = -2 \sum_{q=1}^{2} a_{pq}^2 (s_q \cos 2\phi_{pq} + \omega_q \sin 2\phi_{pq}), \tag{64}$$

and

$$\frac{1}{m_p^2} \frac{\partial m_p}{\partial \phi_{pq}} = 4a_{pq}^2 (s_q \sin 2\phi_{pq} - \omega_q \cos 2\phi_{pq}). \tag{65}$$

When the damping is small, the phases ϕ_{pq} are all near $-\pi/4$ modulo π, so that

$$\phi_{pq} = -\pi/4 + \alpha_{pq}, \tag{66}$$

where $\alpha_{pq} \propto s_q$. Thus,

$$\sin 2\phi_{pq} = \sin(-\pi/2 + 2\alpha_{pq}) = -\cos 2\alpha_{pq} \sim -1, \tag{67}$$

$$\cos 2\phi_{pq} = \cos(-\pi/2 + 2\alpha_{pq}) = \sin 2\alpha_{pq} \sim 2\alpha_{pq} \sim s_q, \tag{68}$$

so that

$$-\frac{1}{m_p^2} \frac{\partial m_p}{\partial \phi_{pq}} \propto s_q. \tag{69}$$

We may show similarly that the sensitivities of the terms of the matrix $\mathbf{K}^{-1}$ are also small, proportional to the real parts of the eigenvalues.

On the other hand, the damping matrix is given by equation (25), so that when **M** is diagonal,

$$b_{pq} = -2m_p m_q \,\mathrm{Re}(\lambda_1^2 y_{p1} y_{q1} + \lambda_2^2 y_{p2} y_{q2}) \tag{70}$$

$$= -2m_p m_q \sum_{j=1}^{2} \{(s_j^2 - \omega_j^2)\cos(\phi_{pj} + \phi_{qj}) + 2\omega_j s_j \sin(\phi_{pj} + \phi_{qj})\} a_{pj} a_{qj}. \tag{71}$$

This equation shows b_{pq} as the product of two terms, the first of which is $m_p m_q$. The sensitivities of m_p and m_q to changes in phase have already been shown to be small. Typical sensitivities of the remaining parts are

$$\frac{\partial}{\partial \phi_{kj}}\left(\frac{b_{11}}{m_1^2}\right) = 4\{(s_j^2 - \omega_j^2)\sin 2\phi_{kj} - \omega_j s_j \cos 2\phi_{kj}\} a_{1j}^2, \tag{72}$$

$$\frac{\partial}{\partial \phi_{kj}}\left(\frac{b_{12}}{m_1 m_2}\right) = 2\{(s_j^2 - \omega_j^2)\sin(\phi_{kj} + \phi_{k'j}) - \omega_j s_j \cos(\phi_{kj} + \phi_{k'j})\} a_{1j} a_{2j}, \tag{73}$$

where the pair of indices (k, k') are either $(1,2)$ or $(2,1)$.

As before, for small damping, the sine terms are approximately (-1), while the cosine terms are of the order of s_1 or s_2. This means that the dominant term in the sensitivity of b_{pq} with respect to ϕ_{jk} is of the order ω_j^2, i.e.,

$$\frac{\partial b_{pq}}{\partial \phi_{kj}} \propto \omega_j^2. \tag{74}$$

These sensitivities are not small, i.e. proportional to the s_j, but are proportional to the squares of the natural frequencies.

6. NUMERICAL SENSITIVITY SIMULATION

We consider a numerical example similar to that found in the experiment:

$$\mathbf{M} = \begin{bmatrix} 4.5 & 0 \\ 0 & 5.0 \end{bmatrix}, \quad \mathbf{B} = \begin{bmatrix} 15 & -5 \\ -5 & 20 \end{bmatrix}, \quad \mathbf{K} = \begin{bmatrix} 2 & -1 \\ -1 & 1.5 \end{bmatrix} 10^5. \tag{75}$$

The exact eigenvalues and eigenvectors are

$$\Lambda = diag\{-1.39 + 122.2\,i,\ -2.28 + 243.9\,i\}, \tag{76}$$

$$\mathbf{Y} = \begin{bmatrix} 0.0124 - 0.0124\,i & 0.0122 - 0.0123\,i \\ 0.0164 - 0.0165\,i & -0.0084 + 0.0083\,i \end{bmatrix}. \tag{77}$$

We note that the damping is not modal because the condition for this to hold, namely $\mathbf{KM}^{-1}\mathbf{B} = \mathbf{BM}^{-1}\mathbf{K}$, is not satisfied. In fact

$$\mathbf{KM}^{-1}\mathbf{B} = \frac{10^5}{18}\begin{bmatrix} 138 & -112 \\ -87 & 128 \end{bmatrix}, \quad \mathbf{BM}^{-1}\mathbf{K} = \frac{10^5}{18}\begin{bmatrix} 138 & -87 \\ -112 & 128 \end{bmatrix}. \tag{78}$$

Both methods, Danek's reconstruction and complex eigenvalues, were used to construct the three matrices **M**, **B**, **K**. Noise was added to all the data according to the formula

$$\hat{x} = x[1 + \alpha r], \tag{79}$$

where r is a random number between -1 and 1, and α corresponds to the noise level. Ten values of α were used, logarithmically spaced between 10^{-2} and 1. The reconstruction errors were quantified by the relative distances:

$$\varepsilon_M = \frac{\|\hat{\mathbf{M}} - \mathbf{M}\|}{\|\mathbf{M}\|}, \quad \varepsilon_B = \frac{\|\hat{\mathbf{B}} - \mathbf{B}\|}{\|\mathbf{B}\|}, \quad \varepsilon_K = \frac{\|\hat{\mathbf{K}} - \mathbf{K}\|}{\|\mathbf{K}\|}, \tag{80}$$

where the norm of the matrices were taken as their greater eigenvalue.

Figures 8–12 show the evolution of the reconstruction errors (%) with respect to the level of noise (%) for matrices **M**, **B**, **K**.

It can be seen that the reconstruction of the damping matrix via Danek's method is very sensitive to the phase of the eigenvectors: a perturbation of 1% leads to an error of nearly 65% ! No other sensitivity exceeds 2%, showing that the eigenvalue reconstructions are much more robust to data uncertainties.

7. EXPERIMENTAL SET-UP

7.1. THE STRUCTURE

The structure is shown in Figure 1. There are two straight beams and one curved beam: beam 1, length 380 mm, section 40×10 mm; beam 2, length 565 mm, section 50×10 mm; beam 3, length 670 mm, section 50×6 mm.

There are two masses, each comprising two blocks, $20 \times 80 \times 80$ mm, bolted to the ends of the beams 1 and 3, and 2 and 3 respectively.

7.2. EXCITATION

The excitation is provided by a light electromagnetic exciter. A coil is attached to mass 1 and placed inside the induction field of a magnet fixed to the ground, as shown in Figure 2. The coil is connected to a signal generator via a power amplifier. A 1 Ω resistance is used to measure the excitation current, which is proportional to the applied force. The proportionality coefficient had been previously determined during a calibration procedure.

7.3. ACCELERATION MEASUREMENT

The two accelerations are measured using Brüel & Kjaer accelerometers (type 4367, mass = 13 g) which are associated with two charge amplifiers B&K (type 2626). The gain of those amplifiers is adjusted such that the output tension is 1 V for an acceleration of $9.81\,\text{m/s}^2$. Due to the particular direction of both excitation and measurements, only in-plane vibrations are considered.

7.4. FEEDBACK DAMPING

Local feedback damping is applied to each beam using a small coil as velocity sensor and a large coil as feedback actuator, one on each side of the beam, as shown in Figure 3. The

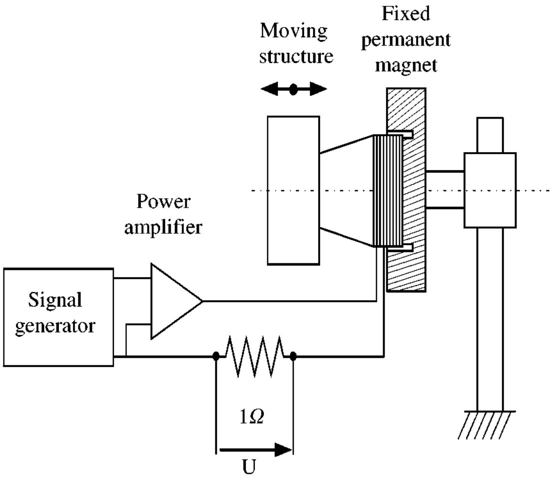

Figure 2. Electromagnetic exciter.

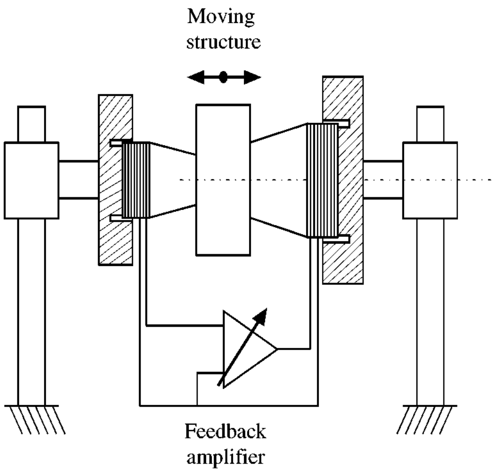

Figure 3. Feedback damping.

TABLE 1

Feedback gains of the nine damping configurations

Configuration	0	1	2	3	4	5	6	7	8
g_1	0	2	5	10	20	25	20	10	25
g_2	0	2	5	10	20	25	2	2	0

tensions coming from each velocity sensor can be amplified separately. Nine different damping configurations were applied. Table 1 gives the corresponding feedback gains g_1, g_2. These gains have to be taken in a qualitative sense. They represent the ratios between the tensions delivered by the velocity sensors and the tensions applied to the collocated actuators, without taking into account the calibration coefficients of sensors and actuators.

7.5. CONSTRAINT

The constraint consists in fixing the mass m_2 to the ground. This is simply done by interposing an iron block between the bottom of the mass and the ground. The height of the block is taken a little bit larger than the gap such that the friction forces are enough to block the mass.

7.6. MEASUREMENTS

All measurements were performed by using a DSP Siglab acquisition set-up connected to a PC. The output of the device was connected to the excitation coil, and three inputs were measured: the excitation current and the accelerations of masses 1 and 2.

Each measurement was performed with the following procedure: (1) random excitation between 0 and 50 Hz; this gave the approximate natural frequencies and 3 dB bandwidths, (2) stepped sine excitation precisely located around each natural frequency.

The Bode plots corresponding to damping configurations 0 and 6 are shown in Figures 4 and 5; the first shows the plot for the unconstrained system, the second for the system with mass 2 blocked. The complex eigenvalues and eigenvectors were extracted by using the linear curve-fitting method of Modan [5]. The real eigenvalues and real eigenvectors were extracted from the complex ones by using the appropriation technique [7]. The technique also extracts the modal damping matrix from the real and complex modes.

8. RESULTS

8.1. COMPLEX EIGENVALUES AND MODES

Table 2 shows the real and imaginary parts of the eigenvalues. Those for the unconstrained system are $\lambda_1 = -s_1 + \mathrm{i}\,\omega_1$, $\lambda_2 = -s_2 + \mathrm{i}\,\omega_2$; that for the constrained system is $\mu_1 = -t_1 + \mathrm{i}\,\sigma_1$. Table 3 shows the eigenvectors; the columns of

$$\mathbf{Y} = \begin{bmatrix} Y_{11} & Y_{12} \\ Y_{21} & Y_{22} \end{bmatrix}$$

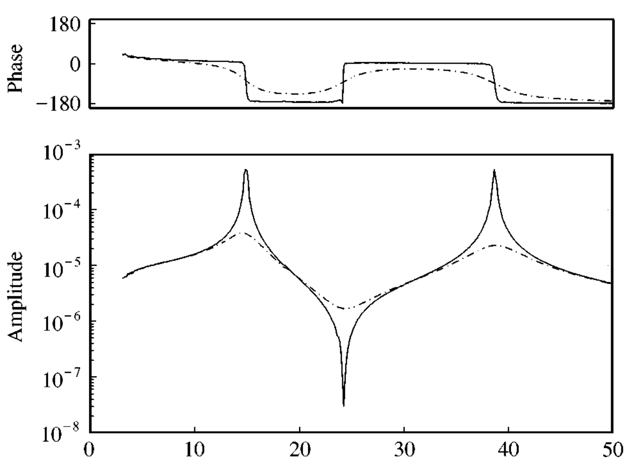

Figure 4. Displacement FRF of the unconstrained system: ——, damping configurations 0; –···–, 6.

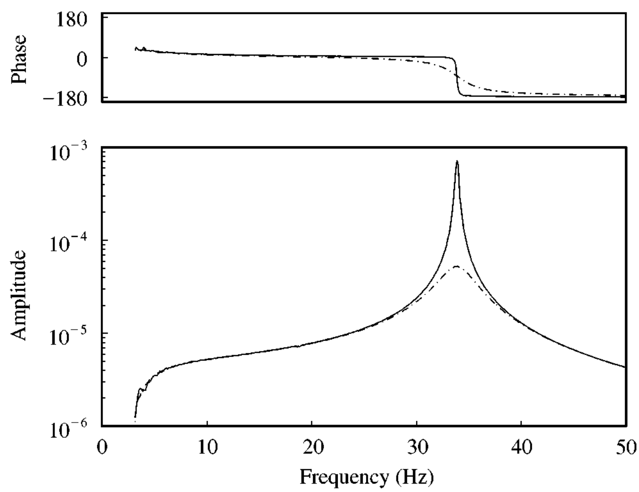

Figure 5. Displacement FRF of the constrained system: ——, damping configurations 0; – · · · –, 6.

TABLE 2

Identified complex eigenvalues

Configuration	s_1	ω_1	s_2	ω_2	t_1	σ_1
0	0·1628	93·49	0·4117	242·4	0·4097	212·7
1	0·8611	93·67	1·373	242·9	0·9524	213·1
2	1·711	93·61	2·748	242·9	1·972	213·1
3	2·984	93·56	4·821	243·0	3·482	213·3
4	5·642	93·37	9·280	243·1	7·069	213·4
5	9·436	92·26	14·91	243·2	10·57	213·6
6	2·330	93·67	6·030	243·1	7·069	213·4
7	1·501	93·64	3·347	243·0	3·482	213·3
8	3·141	93·73	8·627	243·2	10·57	213·6

TABLE 3

Identified complex eigenvectors

Conf.	$_rY_{11}$	$_iY_{11}$	$_rY_{21}$	$_iY_{21}$	$_rY_{12}$	$_iY_{12}$	$_rY_{22}$	$_iY_{22}$
0	0·0148	−0·0101	0·0211	−0·0156	0·0142	−0·0111	−0·0100	0·0081
1	0·0145	−0·0120	0·0205	−0·0184	0·0137	−0·0121	−0·0097	0·0087
2	0·0145	−0·0120	0·0205	−0·0185	0·0135	−0·0124	−0·0096	0·0089
3	0·0145	−0·0121	0·0205	−0·0186	0·0135	−0·0125	−0·0096	0·0090
4	0·0145	−0·0121	0·0205	−0·0187	0·0134	−0·0126	−0·0096	0·0090
5	0·0146	−0·0120	0·0204	−0·0188	0·0133	−0·0128	−0·0096	0·0091
6	0·0143	−0·0123	0·0206	−0·0184	0·0137	−0·0124	−0·0092	0·0093
7	0·0144	−0·0120	0·0205	−0·0183	0·0136	−0·0124	−0·0094	0·0091
8	0·0141	−0·0124	0·0206	−0·0183	0·0137	−0·0123	−0·0090	0·0095

are the eigenvectors of the unconstrained system, and we note

$$Y_{pq} = {}_rY_{pq} + i\,({}_iY_{pq}), \quad p, q = 1, 2. \tag{81}$$

It should be remarked that the feedback damping is very efficient. By comparing the initial structure (configuration 0) with the most damped structure (configuration 5), one can observe that the real parts of the eigenvalues increase, respectively, by a ratio of 58 and 36 for the first and second mode. Such a large amount of damping could not be achieved by using only passive techniques.

8.2. CHECKING THE INEQUALITIES

The quantities $x = s_1^{1/2}$, $y = s_2^{1/2}$, $z = t_1^{1/2}$ should satisfy the inequalities (59) and (60). The angle θ in these equations is determined from the natural frequencies ω_1, ω_2, σ_1 via equation (40). Figure 6(a) shows the sections $y = 0.4117^{1/2} = 0.642$ of the region bounded by equation (59), (60) for damping configuration 0; Figure 6(b) shows the section $y = (8.627)^{1/2} = 2.937$ for configuration 8. In both cases $P(x, y, z)$ lies inside the (shaded) feasible region. Figures 6(a) an 6(b) were constructed from the values of θ computed from the measured values of $\omega_1, \omega_2, \sigma_1$ for the appropriate damping configuration. However, ω_1, ω_2, σ_1 vary only slightly with the damping; they have mean values 93.52, 243.0, 213.4 with standard deviations 0.237, 0.250, 0.276 respectively. Figure 7 shows the three-dimensional (3-D) region constructed from the value of θ computed via equation (40) from the mean values of ω_1, ω_2, σ_1. Again all the points $P(x, y, z)$ lie inside the feasible region.

8.3. THE DANEK ORTHOGONALITY CONDITION

If the measured complex modes are in fact the eigenmodes of a 2 d.o.f. viscously damped system, they should satisfy equation (26). Table 4 shows the value of

$$\eta = \frac{\|\mathrm{Re}(\mathbf{YY}^{\mathrm{T}})\|}{\|\mathbf{YY}^{\mathrm{T}}\|}100. \tag{82}$$

The orthogonality condition is not well satisfied by the measured complex modes. This confirms the view that even with apparently precise measurements the errors in amplitudes and phases of the components of the eigenvectors are considerably greater than those in the eigenvalues; the errors can exceed 5%.

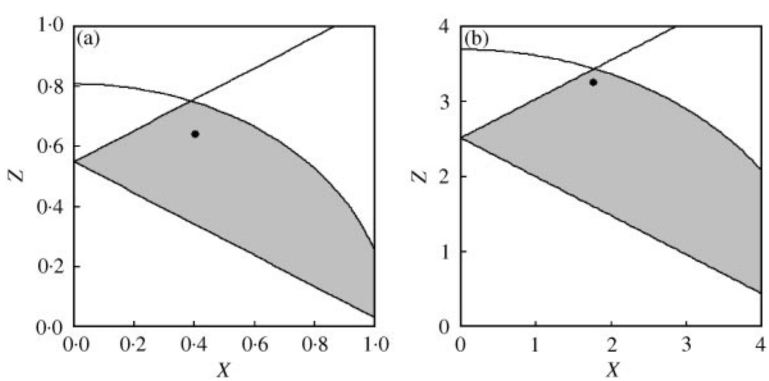

Figure 6. 2D representations of the feasible regions. (a) damping configuration 0, $Y = 0.642$; (b) damping configuration 9, $Y = 2.94$.

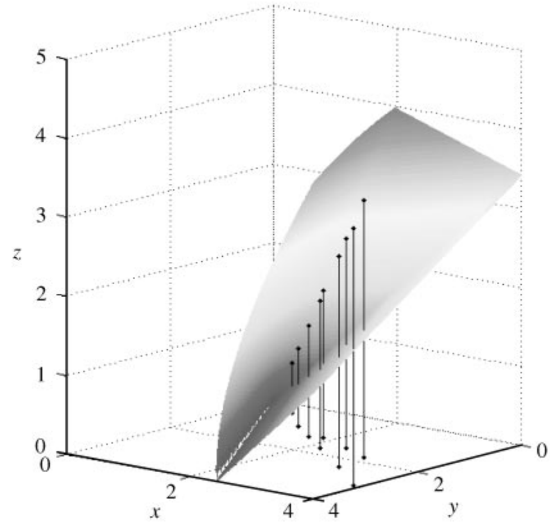

Figure 7. 3D representation of the feasible region.

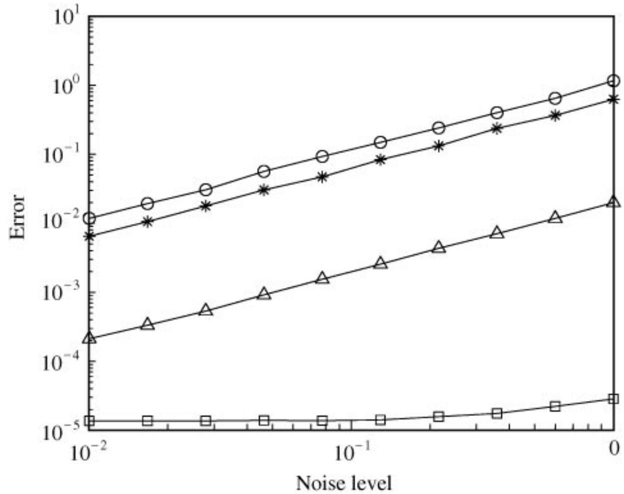

Figure 8. Sensitivity of the mass matrix, Danek reconstruction: □, sensitivity to the real part of the eigenvalues; $*$, sensitivity to the imaginary part of the eigenvalues; ○, sensitivity to the magnitude of the eigenvectors; △, sensitivity to the phase of the eigenvectors.

8.4. THE RECONSTRUCTED MATRICES

Table 5 shows the matrices **M**, **K** computed from the real eigenvalues and real eigenvectors, and the damping matrix **B** computed from the modal damping parameters in equations (8) and (6). Table 6 shows the matrices **M**, **B**, **K** computed by Danek's reconstruction.

Omitting in both cases the outlier configuration 0, the mean mass and stiffness matrices are

$$\mathbf{M}_M = \begin{bmatrix} 4.385 & 0.391 \\ 0.391 & 4.462 \end{bmatrix}, \quad \mathbf{K}_M = \begin{bmatrix} 1.775 & -0.912 \\ -0.912 & 1.033 \end{bmatrix} 10^5, \tag{83}$$

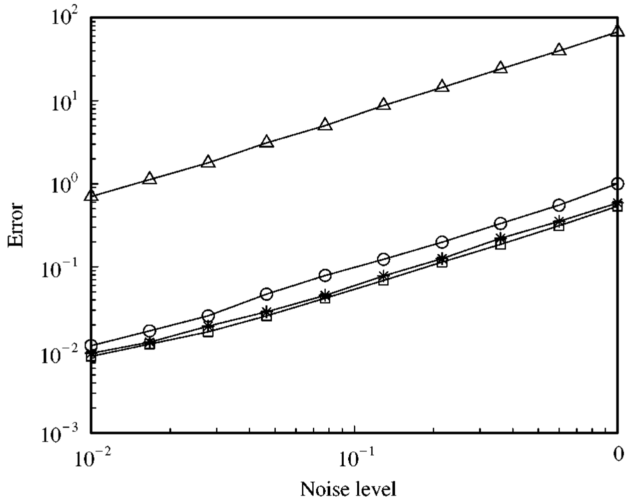

Figure 9. Sensitivity of the damping matrix, Danek reconstruction: □, sensitivity to the real part of the eigenvalues; ∗, sensitivity to the imaginary part of the eigenvalues; ○, sensitivity to the magnitude of the eigenvectors; △, sensitivity to the phase of the eigenvectors.

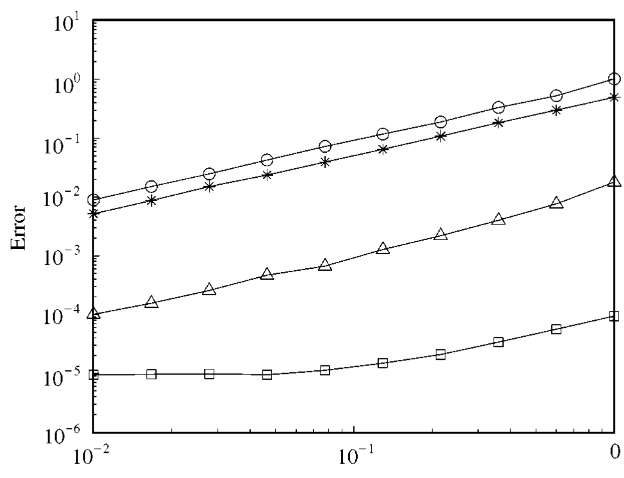

Figure 10. Sensitivity of the stiffness matrix, Danek reconstruction: □, sensitivity to the real part of the eigenvalues; ∗, sensitivity to the imaginary part of the eigenvalues; ○, sensitivity to the magnitude of the eigenvectors; △, sensitivity to the phase of the eigenvectors.

$$\mathbf{M}_D = \begin{bmatrix} 4.418 & 0.409 \\ 0.409 & 4.485 \end{bmatrix}, \quad \mathbf{K}_D = \begin{bmatrix} 1.780 & -0.914 \\ -0.914 & 1.035 \end{bmatrix} 10^5. \tag{84}$$

The standard deviations of these matrices are

$$sd(\mathbf{M}_M) = \begin{bmatrix} 0.027 & 0.010 \\ 0.010 & 0.029 \end{bmatrix}, \quad sd(\mathbf{K}_M) = \begin{bmatrix} 0.012 & 0.006 \\ 0.006 & 0.008 \end{bmatrix} 10^5, \tag{85}$$

$$sd(\mathbf{M}_D) = \begin{bmatrix} 0.024 & 0.016 \\ 0.016 & 0.022 \end{bmatrix}, \quad sd(\mathbf{K}_D) = \begin{bmatrix} 0.014 & 0.007 \\ 0.007 & 0.007 \end{bmatrix} 10^5. \tag{86}$$

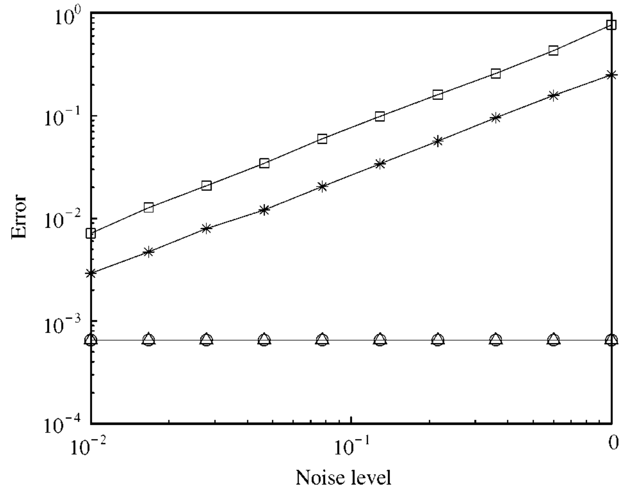

Figure 11. Sensitivity of the damping matrix, eigenvalues reconstruction: □, sensitivity to the real part of the eigenvalues; $*$, sensitivity to the imaginary part of the eigenvalues; ○, sensitivity to the magnitude of the eigenvectors; △, sensitivity to the phase of the eigenvectors.

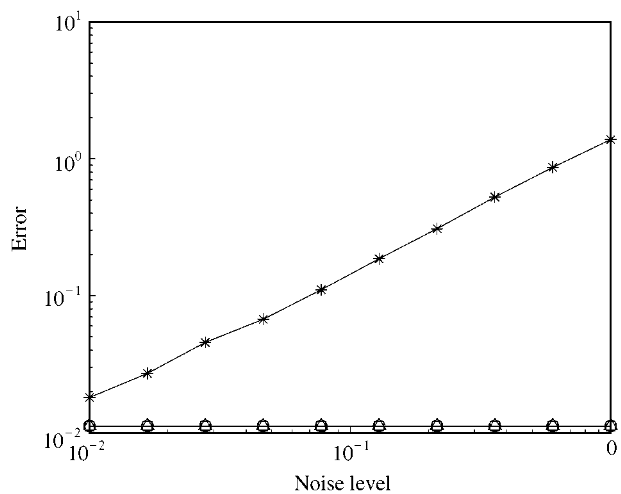

Figure 12. Sensitivity of the stiffness matrix, eigenvalues reconstruction: □, sensitivity to the real part of the eigenvalues; $*$, sensitivity to the imaginary part of the eigenvalues; ○, sensitivity to the magnitude of the eigenvectors; △, sensitivity to the phase of the eigenvectors.

An inspection of the damping matrices in Tables 5 and 6 will show that there is no correlation between the two sets. The Danek values are non-sensical. Even omitting configuration 0, we see that the damping matrices do not steadily increase as the damping steadily increases in configurations 1–5. Table 7 shows the matrices **B** and **K** computed from the eigenvalue reconstruction method. Here we have used the mass matrix **M** computed from the Danek reconstruction to give **L** from the factorization $\mathbf{M} = \mathbf{L}\mathbf{L}^{\mathrm{T}}$. The mean and the standard deviation of the stiffness matrix are

$$\mathbf{K}_E = \begin{bmatrix} 1.822 & -0.898 \\ -0.898 & 1.000 \end{bmatrix} 10^5, \quad sd(\mathbf{K}_E) = \begin{bmatrix} 0.013 & 0.056 \\ 0.056 & 0.006 \end{bmatrix} 10^5. \tag{87}$$

TABLE 4

Danek orthogonality condition

Conf.	0	1	2	3	4	5	6	7	8
η	31·64	13·61	13·40	12·53	12·21	12·26	13·00	13·44	12·55

TABLE 5

Reconstructed matrices using modal method

Conf.	**M**		**B**		$\mathbf{K}/10^5$	
0	4·63	0·50	3·11	− 0·80	1·84	− 0·93
	0·50	4·74	− 0·80	2·37	− 0·93	1·08
1	4·43	0·36	10·63	− 1·34	1·80	− 0·93
	0·36	4·44	− 1·34	9·12	− 0·93	1·04
2	4·34	0·36	20·76	− 2·65	1·77	− 0·91
	0·36	4·44	− 2·65	18·05	− 0·91	1·03
3	4·27	0·33	36·06	− 4·64	1·76	− 0·91
	0·33	4·42	− 4·64	31·80	− 0·91	1·03
4	4·21	0·27	68·81	− 9·99	1·77	− 0·93
	0·27	4·44	− 9·99	61·18	− 0·93	1·04
5	4·11	0·21	110·2	− 15·18	1·76	− 0·94
	0·21	4·49	− 15·18	102·9	− 0·94	1·06
6	4·25	0·34	40·59	− 12·21	1·76	− 0·91
	0·34	4·47	− 12·21	30·81	− 0·91	1·04
7	4·32	0·35	23·47	− 5·81	1·77	− 0·92
	0·35	4·47	− 5·81	18·52	− 0·92	1·04
8	4·25	0·31	57·79	− 18·76	1·78	− 0·93
	0·31	4·50	− 18·76	43·13	− 0·93	1·05

8.5. THE RECALCULATED EIGENVALUES AND EIGENVECTORS

The complex eigenvalues and eigenvectors were recalculated from the eigenvalue equation (14). Table 8 shows the percentage errors ε_R, ε_I defined by

$$\varepsilon_R = \frac{|s_j - \tilde{s}_j|}{s_j} 100, \quad \varepsilon_I = \frac{|\omega_j - \tilde{\omega}_j|}{\omega_j} 100 \tag{88}$$

for each mode and for the three methods, modal (M), Danek (D) and eigenvalues (E).

Clearly, the Danek reconstruction is completely unreliable for measuring the real parts of the eigenvalues from the reconstructed matrices. The modal method is reasonably reliable. Of course, the errors in the values computed from the eigenvalue reconstruction depend only on the accuracy of the numerical linear algebra; they do not depend on the matrix **M** used in the factorization $\mathbf{M} = \mathbf{L}\mathbf{L}^{\mathrm{T}}$ because the factors $\mathbf{L}$, $\mathbf{L}^{\mathrm{T}}$ do not affect the eigenvalues:

$$\mathbf{M}\lambda^2 + \mathbf{B}\lambda + \mathbf{K} = \mathbf{L}(\mathbf{I}\lambda^2 + \mathbf{C}\lambda + \mathbf{A})\mathbf{L}^{\mathrm{T}}. \tag{89}$$

We computed the modal assurance criterion (MAC) and the modal scale factor (MSF) for the modes calculated by all three methods but found that they were all almost 1·0; there was no significant differences between the three sets of results.

TABLE 6

Reconstructed matrices using Danek's method

Conf.	M		B		$\mathbf{K}/10^5$	
0	4·88	0·64	252·3	− 25·62	1·92	− 0·95
	0·64	5·04	− 25·62	175·4	− 0·95	1·11
1	4·46	0·38	125·0	− 21·66	1·81	− 0·93
	0·38	4·51	− 21·66	72·69	− 0·93	1·05
2	4·43	0·40	109·4	− 7·59	1·79	− 0·92
	0·40	4·49	− 7·59	71·59	− 0·92	1·04
3	4·40	0·41	111·8	− 6·60	1·77	− 0·91
	0·41	4·47	− 6·60	81·27	− 0·91	1·03
4	4·41	0·41	135·0	− 6·37	1·78	− 0·91
	0·41	4·46	− 6·37	105·5	− 0·91	1·03
5	4·41	0·43	166·0	− 3·44	1·77	− 0·91
	0·43	4·46	− 3·44	142·2	− 0·91	1·03
6	4·39	0·42	137·0	− 1·49	1·76	− 0·91
	0·42	4·48	− 1·49	56·83	− 0·91	1·03
7	4·43	0·42	117·0	− 3·79	1·78	− 0·91
	0·42	4·51	− 3·79	61·09	− 0·91	1·04
8	4·41	0·40	160·7	− 0·46	1·78	− 0·91
	0·40	4·50	− 0·46	53·32	− 0·91	1·04

TABLE 7

Reconstructed matrices using eigenvalues method

Conf.	B		$\mathbf{K}/10^5$	
0	3·77	− 0·54	1·91	− 0·95
	− 0·54	1·66	− 0·95	1·12
1	7·95	− 2·35	1·85	− 0·91
	− 2·35	11·56	− 0·91	1·01
2	16·38	− 4·40	1·83	− 0·90
	− 4·40	22·34	− 0·90	1·00
3	28·65	− 7·50	1·81	− 0·89
	− 7·50	38·63	− 0·89	0·99
4	58·80	− 13·52	1·82	− 0·90
	− 13·52	70·04	− 0·90	0·99
5	86·85	− 22·73	1·81	− 0·89
	− 22·73	122·9	− 0·89	0·99
6	60·64	− 4·04	1·81	− 0·89
	− 4·04	11·57	− 0·89	1·00
7	29·90	− 3·22	1·82	− 0·90
	− 3·22	12·33	− 0·90	1·01
8	91·45	− 4·77	1·82	− 0·90
	− 4·77	10·76	− 0·90	1·00

9. CONCLUSION

This experimental–theoretical paper develops three aspects of the inverse identification problem.

TABLE 8

Percentage errors on the recalculated complex eigenvalues

Method		**M**		**D**		**E**	
Conf.	Mode	ε_R	ε_I	ε_R	ε_I	ε_R	ε_I
0	1	9·97	0·05	9573	1·47	0·0000	0·0001
	2	4·83	0·11	6924	0·69	0·0000	0·0001
1	1	1·63	0·15	726	0·40	0·0007	0·0038
	2	1·17	0·48	1031	0·19	0·0005	0·0020
2	1	1·27	0·90	361	0·57	0·0022	0·0155
	2	0·92	1·56	363	0·14	0·0014	0·0076
3	1	3·24	0·35	194	0·78	0·0064	0·0473
	2	0·90	0·25	177	0·18	0·0040	0·0233
4	1	4·14	0·41	100	1·27	0·0137	0·1751
	2	1·04	0·04	74	0·25	0·0083	0·0806
5	1	5·84	0·06	60	2·03	0·0752	0·4753
	2	1·31	0·09	34	0·24	0·0476	0·2295
6	1	2·60	0·14	259	0·66	0·0303	0·0100
	2	1·12	0·22	129	0·33	0·0117	0·0517
7	1	2·83	0·23	414	0·52	0·0032	0·0108
	2	0·99	0·20	273	0·20	0·0014	0·0115
8	1	2·36	0·12	186	0·78	0·0823	0·0029
	2	1·24	0·29	78	0·45	0·0300	0·1220

The first aspect concerns the introduction of controlled and adjustable viscous damping in a continuous simple structure, initially very lightly damped, by an electro-dynamic collocated feedback. The domain of variation of the real parts of the two first complex eigenvalues is significantly large. The ratio of this variation is about 60 for the first mode.

The second aspect concerns the construction, by three different methods, of a discrete condensed model **M**, **B**, **K** of order 2, admitting as complex eigensolutions the two first eigensolutions observed on the continuous structure. The comparison of the results of these three methods illustrates their capabilities. These results are justified by a sensitivity analysis.

The last aspect exploits the possibilities of experimental control of viscous damping with the aim of validating the analytical developments concerning the domain of variation of the real parts of the first two complex eigenvalues and of the complex eigenvalue of the constrained system.

REFERENCES

1. M. I. FRISWELL and J. E. MOTTERSHEAD 1995 *Finite Element Model Updating in Structural Dynamics*. Dordrecht: Kluwer Academic Publishers.
2. J. E. MOTTERSHEAD and M. I. FRISWELL 1993 *Journal of Sound and Vibration* **167**, 347–375. Model updating in structural dynamics.
3. T. K. CAUGHEY and M. E. J. KELLY 1965 *Journal of Applied Mechanics* **32**, 583–588. Classical normal modes in damped linear dynamic systems.
4. G. M. L. GLADWELL 2000 *Journal of Sound and Vibration* **240**, 203–217. On the reconstruction of a damped vibrating system from two complex spectra I; theory.

5. J. PIRANDA 1994 *Analyse modale et recalage de modèle*. Habilitation à Diriger les Recherches, Université de Franche-Comté
6. O. DANEK 1979 *Strojnicky casopis* **30**, 650–657 Inversion formulas for non-conservative systems (in Czech).
7. E. FOLTÊTE 1998 *Doctoral Thesis*, *Université de Franche-Comté. Identification modale de structures linéaires et faiblement non-linéaires.*